

Preparation of Porous Poly(3-hexylthiophene) by Freeze-Dry Method and Its Application to Organic Photovoltaics

Ping-Tsung Huang, Yao-Sheng Chang, Cheng-Wei Chou

Department of Chemistry, Fu Jen Catholic University, Taipei 24205, Taiwan

Received 4 October 2010; accepted 11 January 2011

DOI 10.1002/app.34132

Published online 20 April 2011 in Wiley Online Library (wileyonlinelibrary.com).

ABSTRACT: Poly(3-hexylthiophene)(P3HT) with a micro-porous network structure was prepared from a 1% *p*-xylene solution by freeze-dry method. Scanning electron microscopy (SEM) showed P3HT molecules formed swollen gel-like structures with different extent of compactness depending on the length of the aggregation period. Absorption spectrum of this P3HT film showed a characteristic peak at 620 nm, which indicated a high degree of order between polymer chains. Photoluminescence (PL) of this highly ordered P3HT film appeared at 712 nm revealing large extent of π - π stacking between P3HT molecules in the freeze-dry film. Both absorption and photoluminescence results indicated that the original aggregated states of P3HT molecules in gel form had

been preserved throughout the freeze-dry operation. X-ray diffraction of the annealed samples showed a strong characteristic peak for the side chain aggregation at $2\theta = 5.1^\circ$, which proved that the freeze-dry film was with highly order structure. The interconnected and highly ordered P3HT film is used in the study of organic photovoltaics (OPV) after applying an *n*-type semiconductor to the surface of the dry porous fibers. A prototype OPV device with power conversion efficiency of 1.47% was prepared by this method. © 2011 Wiley Periodicals, Inc. *J Appl Polym Sci* 122: 233–240, 2011

Key words: P3HT; gel; freeze-dry; morphology; organic photovoltaics

INTRODUCTION

Poly(3-hexylthiophene)(P3HT) has been widely studied for many organic electronic applications such as OPV because of its high mobility character among many other *p*-type semiconducting polymers.^{1–3} Morphology of P3HT films are affected by many factors such as thermal treatment,^{5,6} molecular weight,^{7–9} regioregularity,^{10,11} end group,¹² solvent selection,^{13–15} and solvent evaporation rate.^{16,17} Among these factors, selection of an appropriate solvent and thermal treatment conditions are most crucial to the end properties of P3HT and related organic electronic devices. A common practice for OPV sample preparation is spin-coating of the P3HT/PCBM solution on a substrate followed by thermal treatment to induce a local order structure by aggregation of polymer side chains in a solid state. Brabec and coworkers^{13,15} showed that aggregation of P3HT could be improved by using a high boiling point solvent because of better organization of the polymer chain during the evaporation of the

solvent. Researchers⁴ showed that annealed P3HT film resulted in better side-chain aggregation that could be identified by X-ray analysis. Mobility of the annealed P3HT was enhanced due to the formation of order structure.⁶

Thermal treatment of P3HT/PCBM film not only affects carrier mobility through order domain formation, but also affects the morphology of the bi-continuous phase required for the OPV. Study¹⁸ showed that the formation of a bi-continuous phase in bulk heterojunction morphology greatly improved carrier transport in *n*-type material and resulted in higher power conversion efficiency. Although a bi-continuous phase can be created in a bulk heterojunction manner, many problems such as traps formation and domain size control exist in the heterojunction region. These problems are a result of the incompatibility between the *p*-type and the *n*-type materials.^{19–21} Therefore, an efficient method for the creation of a bi-continuous phase has become an important issue in the performance and long-term stability of OPV.

In addition to the solvent selection and thermal treatment methods, researchers^{22,23} found that power conversion efficiency of polymer solar cells was improved by the separation of aggregated fibers from solution. The precipitated fiber showed strong absorption at 610 nm that originated from aggregation of P3HT molecules. It had also been reported that exposing P3HT/PCBM films to solvent vapor along

Correspondence to: P.-T. Huang (073802@mail.fju.edu.tw).
Contract grant sponsor: National Science Council of Taiwan; contract grant number: NSC-97-2113M-030-003.
Contract grant sponsor: Academia Sinica.

with a subsequent thermal annealing step (referred to as the solvent annealing step) led to an improvement in efficiency.^{16,24} Meanwhile, another study demonstrated that better device performance was obtained by exposing the dried film to solvent vapor.²⁵

All the above studies have demonstrated the profound effect of the aggregation process and continuous phase formation on the physical properties of P3HT, as well as its effect to the performance of organic solar cell.

The blend of regioregular P3HT as the electron donor and [6,6]-phenyl-C₆₁ butyric acid methyl ester (PCBM) as the electron acceptor is the most common active layer system studied for the OPV, and has achieved power conversion efficiency of 4–5%.^{10,26} Thermal annealing of P3HT/PCBM bulk heterojunction devices is a critical step for improving their efficiency^{1,27} and a relatively high temperature ranging from 120 to 150°C is often used.^{28,29} Recently, Su and coworkers³⁰ had reported on the morphological and optical properties of bulk-heterojunction P3HT/PCBM film by means of scanning probe microscopy equipped with near-field spectroscopy (SNOM), and had suggested an optimal annealing process at 140°C for 30 min. Wei and coworkers³¹ investigated the morphologies of P3HT/PCBM active layer in bulk-heterojunction solar cells annealed at various temperatures by simultaneously applying small-angle X-ray scattering (GISAXS) and wide-angle X-ray diffraction (GIWAXD) techniques, and found that the device exhibited the optimal performance under annealing at 150°C for 15 min. In addition, many different treatment conditions^{1,2,5,27–29,32} were conducted to the P3HT/PCBM layer to control P3HT/PCBM layer with different morphologies and performance.

Currently, most researches use high boiling point solvents such as chlorobenzene and *o*-dichlorobenzene to prepare P3HT/PCBM solution because less aggregation occurs in these solvents. Thermal annealing of the spin-coating film results in improved P3HT organization and higher power conversion efficiency. However, as mentioned earlier, the discrepancy in thermal annealing process leads to different results in device performance because of the uncontrollable phase separation process. It will be very interesting if an OSC device can be prepared by fixing the morphology of a *p*-type semiconductor and thermal annealing is conducted before applying a *n*-type material to the surface of the *p*-type semiconductor so that a bicontinuous phase is formed. We found this goal could be achieved by using a solvent such as *p*-xylene that would create different aggregation states of P3HT in solution followed by a freeze-dry method reported in the present study.

This article presents the results of the formation of a 3D network structure of P3HT aggregates prepared

by a freeze-dry process. The effect of the aggregation period on the morphology of the P3HT film prior to the freeze-dry process on the morphology of the P3HT film was examined. Morphologies of both the annealed and nonannealed sample films were investigated, along with a parallel study on the samples prepared by spin-coating process. Scanning electron microscopy (SEM), UV–VIS absorption spectra, photoluminescence spectra, and X-ray diffraction analyses were employed to elucidate the aggregation behaviors of P3HT. Finally, a prototype P3HT/[60]PCBM-based device was fabricated.

EXPERIMENTAL

Materials

P3HT was synthesized by GRIM's method.³³ The synthesized polymer has a M_n of 18,000, and a polydispersity index (PDI) of 2.45. NMR analysis³⁴ showed that the regioregularity of the synthesized P3HT was 93%. A solution of 1% P3HT in *p*-xylene (fp. 12°C, bp 138°C) was prepared by mixing 0.1 g of the P3HT sample with 9.9 g of *p*-xylene (ACS grade, purchased from Aldrich) in an orbital shaker at 70°C for overnight before the freeze-dry process and other measurements.

Sample preparation

The freshly prepared P3HT solution was allowed to stand at 25°C for aggregation for certain periods of time to generate specific aggregation states. The P3HT solution was dropped onto a quartz plate and moved to a copper plate which was cooled to –70°C with a temperature controller. The sample was quenched at that temperature for 5 min. The quenched sample was then quickly transferred to a precooled (–50°C) lab-made temperature controller that was filled with coolant. The quenched sample and temperature controller was then moved to the freeze-dryer (Model: Eyela FDU-2200) and sublimed at –30°C under 1×10^{-4} torr for 2 h to remove *p*-xylene before measurement or thermal annealing treatment. Thermogravimetric analysis (TGA) showed no residual solvent (bp = 138°C for *p*-xylene) in the film at temperature below 200°C for the sample film prepared by the freeze-dry process (Fig. 1).

Device fabrication

The device was fabricated on an ITO substrate with sheet resistance of 12 Ω . The substrate was cleaned in an ultrasonic machine with isopropyl alcohol and deionized water following by treatment with O₂ plasma. A 800-Å layer of poly(3,4-ethylenedioxythiophene) : poly(styrene sulfonate) (PEDOT: PSS; Baytron AI4083) was coated on the ITO substrate and

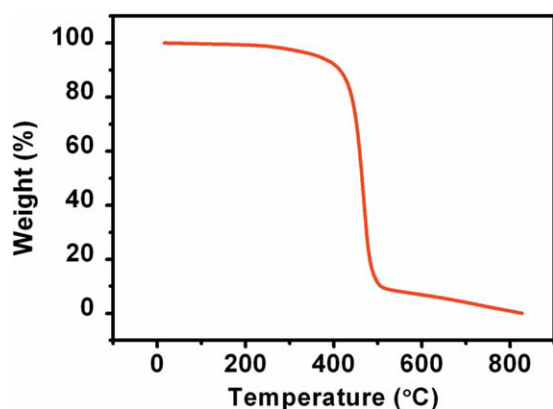


Figure 1 Thermogravimetric analysis of freeze-dry P3HT film under N_2 . [Color figure can be viewed in the online issue, which is available at wileyonlinelibrary.com.]

dried at 200°C for 5 min under N_2 atmosphere. A 1000 Å P3HT film was coated and freeze-dried as described in the sample preparation section followed by annealing at 150°C for 30 min. A 1.0% PCBM solution in dichloromethane was coated on P3HT by using blade coater. The dichloromethane solvent dried in a few minutes and dried P3HT/PCBM film was coated with Ca (50 Å)/Al(2000 Å) film as cathode by a thermal evaporator under 1.0×10^{-6} torrs.

Characterization

The molecular weight of P3HT was measured by Viscotek DM400/LR40 Gel Permeation Chromatography (GPC) using standard polystyrene as a reference. Regioregularity was analyzed by Bruker AV-300 Nuclear Magnetic Resonance. UV-visible absorption measurements were carried out with a Shimadzu UV-21011C spectrometer. Photoluminescence spectra were taken using a Fluorolog, Horiba Jobin Yvon Fluorometer. X-ray study was conducted with an X-ray spectrometer model PANalytical PW3040/60 X'Pert Pro. The morphology of the microporous structure was studied using a Hitachi S-3000N SEM. TGA thermogram was performed on a Perkin-Elmer TGA-7. Device performance was measured by using a calibrated solar simulator (300 Watts Xenon lamp) equipped with a KG-3 filter as light source at AM1.5G conditions (100 mW cm^{-2}).

RESULTS AND DISCUSSION

3D network formation

Various factors affecting the aggregation of P3HT in solution have been investigated by many researchers as mentioned in the Introduction section. Additionally, solution concentration³⁵ and temperature of aggregation³⁶ also affect aggregation of P3HT. To prepare P3HT films with different extent of aggrega-

tion, we used the same P3HT sample in 1% *p*-xylene solution at 25°C so that aggregation time became a controlling factor for the extent of aggregation. The sample was quenched at -70°C and solvent was sublimed at -30°C as described in the sample preparation section. In this manner, a minimal amount of thermal energy was required to remove the solvent and, thus, the state of aggregation of the P3HT molecules in solution could be maintained throughout the entire process. Figure 2 showed the SEM image of P3HT obtained from the freeze-dry method with an aggregation period of 60 min. The SEM microgram indicated that a network structure of P3HT molecules was formed, and the network was interconnected by fibers with a width of about $\sim 1\text{--}2 \mu\text{m}$ at an aggregation period of 60 min.

To investigate the effect of aggregation time on the formed dried films, different aggregation intervals were employed prior to the freeze-dry process. Figure 3 showed the SEM micrograms of the P3HT films prepared at different aggregation intervals. As shown in Figure 3(a) (as-prepared solution, minor aggregation process), P3HT molecules formed a partially interconnected structure of $\sim 0.2\text{--}0.3 \mu\text{m}$ in width. As depicted in Figure 3(b–d), the dimension of aggregated P3HT increased from about $0.2\text{--}0.3 \mu\text{m}$ for an as-prepared solution [Fig. 3(a)] to about $\sim 1\text{--}2 \mu\text{m}$ following an aggregation period of 30 min at 25°C. By applying the freeze-dry process, we were able to generate a porous network structure of P3HT with varying gel thickness simply by controlling the length of the aggregation time.

Polar solvents with high boiling points are often used in P3HT/PCBM film preparation because they allow better P3HT molecular organization during solvent evaporation. This enables an improvement in the carrier mobility of the annealed film that

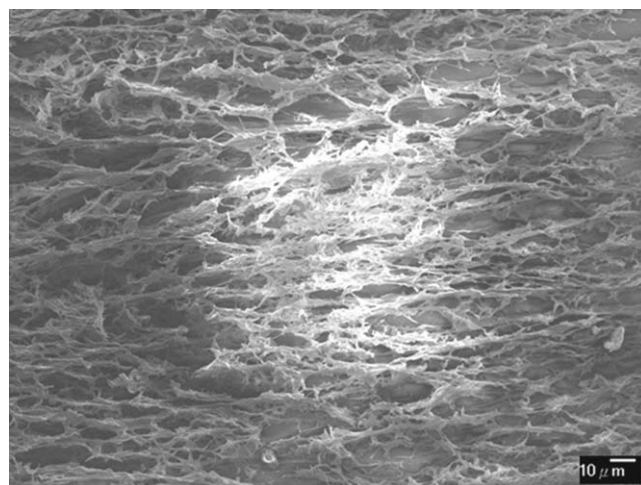


Figure 2 SEM micrograph of a 3-D network structure of P3HT prepared from 1% *p*-xylene solution by the freeze-dry method (proceed with an aggregation period of 60 min).

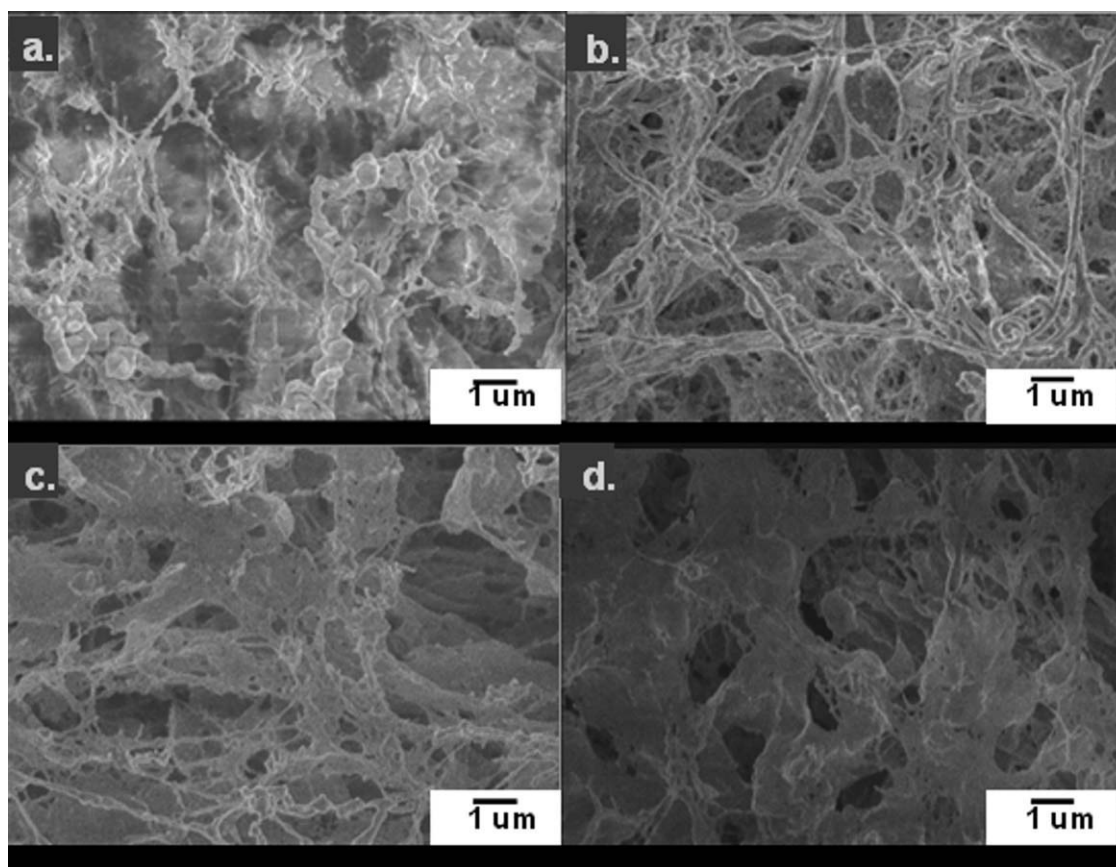


Figure 3 SEM micrographs of 3-D microporous structures of P3HT by freeze-dry method with differing aggregation times: (a) as-prepared solution (0 min), (b) 10 min, (c) 20 min, (d) 30 min.

produces organic solar cells with higher power conversion efficiency. However, the residual solvent content of the spun films is inconsistent from batch to batch because of issues such as temperature, humidity, spin rate, and spin time. The residual solvent acts as a plasticizer for P3HT and lowers its glass transition temperature (T_g). The spun P3HT films exhibit different initial T_g s for different batches owing to the difference in the content of residual solvent. Therefore, it will be very difficult to obtain P3HT/PCBM films with a similar morphology even when similar experimental processes, such as the same annealing temperature and annealing time, are conducted. With the freeze-dry process, porous network of P3HT is formed by controlling its aggregation time in solution and solvent is removed with no additional thermal energy. Therefore, P3HT with a similar aggregation state can be created in a much more controllable way.

Photophysical analysis

P3HT molecules with featured different absorption bands at 530, 560, and 600 nm, are primarily caused by different molecular arrangements that change the extent of π - π^* absorption as reported in the liter-

ature.^{37–39} When allowing the P3HT solution to stand at 25°C for aggregation before freeze-dry treatment, the resultant films consisted of different sizes of P3HT aggregates depending on the length of the aggregation period (Fig. 3). The absorption spectra of these films were distinct from one to another. The spectrum of a freeze-dry sample without an aggregation process showed a strong absorption shoulder at 600 nm (Curve a, Fig. 4), which was similar to that prepared from a spin-coating process (Curve a, Fig. 6) with the noted exception that the intensity of the freeze-dry sample was higher. As the aggregation time increased, this absorption band made a pronounced shift to 613 and 620 nm, respectively, with 20 and 40 min aggregation periods, as shown in Figure 4 (Curves b and c). These results indicated that a better alignment (and/or packaging) of the thiophene moieties existed in the samples prepared by a freeze-dry method, while not in that using a spin-coating process. Figure 4 also revealed that the intensities of the absorption bands at ~ 530 and 560 nm were descended and the band at ~ 620 nm ascended gradually as we prolonged the aggregation period. The band at ~ 620 nm, corresponding to a long-range ordering structure of P3HT, became the maximum absorption band, and a new shoulder

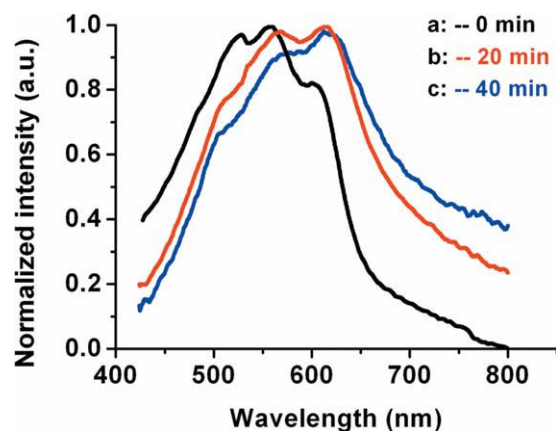


Figure 4 UV-visible spectra of P3HT film prepared by the freeze-dry method with different aggregation times: (a) as-prepared solution (0 min), (b) 20 min, (c) 40 min. [Color figure can be viewed in the online issue, which is available at wileyonlinelibrary.com.]

band appeared at ~ 570 nm, which arose from the original absorption bands at 530 and 560 nm, as the aggregation process was extended to 40 min (Curve c versus curves a and b, Fig. 4). In addition, as shown in Figure 4, the absorption spectra of the films prepared with either 20 or 40 min of aggregation period were quite similar to one another. This indicated that all the freeze-dry samples maintained similar packing structures with the exception of the size of the aggregated gel, as shown in the SEM micrograms in Figure 3.

When the freeze-dry films were annealed at 150°C for 30 min, all these annealed films displayed an almost identical absorption spectra, as shown in Figure 5. The absorption bands located at 570 and 620 nm were nearly the same for all the annealed samples regardless of the difference in the length of the

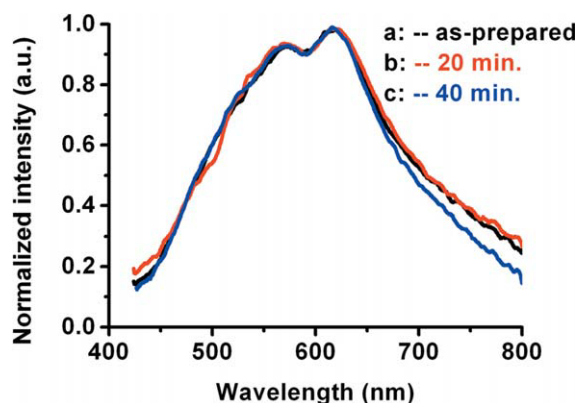


Figure 5 UV-visible spectra of P3HT film prepared by the freeze-dry method with different aggregation time periods: (a) as-prepared solution (0 min), (b) 20 min, (c) 40 min, followed by thermal annealing at 150°C for 30 min. [Color figure can be viewed in the online issue, which is available at wileyonlinelibrary.com.]

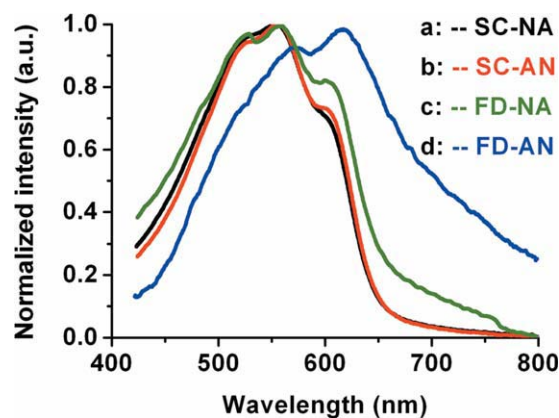


Figure 6 Comparison of UV-vis spectra of nonannealed (NA) and annealed (AN) P3HT films prepared by the spin-coating (SC) and the freeze-dry (FD) methods, respectively. (a) SC-NA film, (b) SC-AN film, (c) FD-NA film, (d) FD-AN film. [Color figure can be viewed in the online issue, which is available at wileyonlinelibrary.com.]

aggregation. These results strongly suggested that a loosely interdigital packing structure had been formed during the aggregation period, which turned into a more compact aggregated structure after thermal annealing treatment.

Figure 6 showed comparisons of the absorption spectra for spin-coating and freeze-dry samples as well as that of the nonannealed and the annealed film samples. Both spin-coating films (annealed and nonannealed) exhibited similar absorption bands at 530, 560, and 600 nm (Curves a and b, Fig. 6). All these absorption bands also appeared in the spectrum of the nonannealed freeze-dry film prepared without an aggregation period (Curve c, Fig. 6) with the noted exception that the intensity of the absorption at 600 nm was slightly more intense. This result indicated that the nonannealed freeze-dry film (prepared without an aggregation period) exhibited a higher degree of order of molecular organization between thiophene units as comparing with that of the spin-coating film that had been annealed at 150°C for 30 min. On the other hand, when the freeze-dry film was annealed under the same conditions, the three original absorption bands shifted to 570 and 620 nm (curves d in Fig. 6).

As reported in literature,⁴⁰ the relative intensity between the shoulder and the main peak revealed information about ordering of the crystallized P3HT. As seen in the case of spin-coating samples, the ratio of intensity at 600 and 560 nm (I_{600}/I_{560}) was 0.729 for both annealed and nonannealed samples. The ratio of I_{600}/I_{560} was 0.824 for the nonannealed freeze-dry film with no aggregation process. With prolonged aggregation time (such as 40 min of aggregation period), the ratio of intensity at 620 and 570 nm (I_{620}/I_{570}) was ~ 1.073 (Curve c, Fig. 4). Furthermore, it is very interesting to note that all the

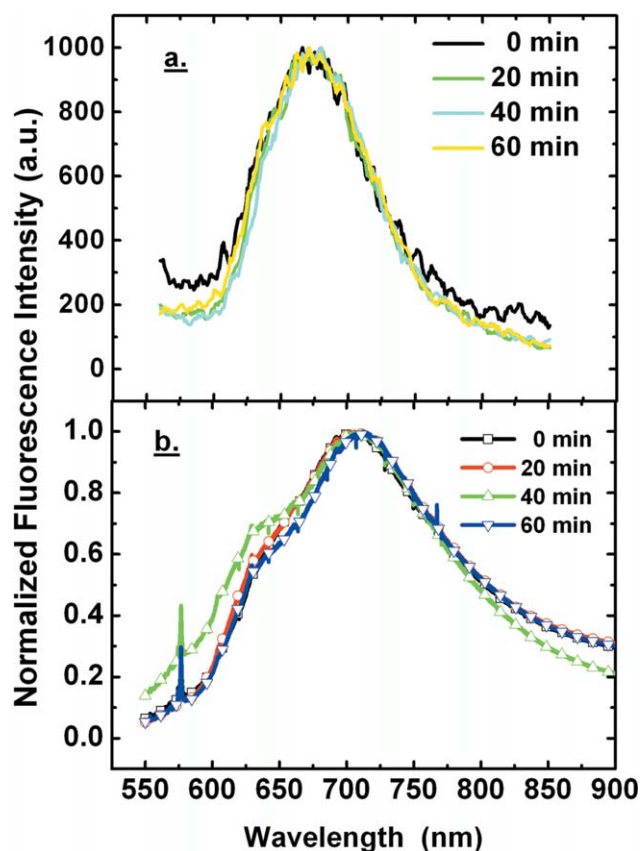


Figure 7 Photoluminescence spectra of P3HT films prepared by: (a) spin coating process and (b) freeze-dry process. All film samples were annealed at 150°C for different time periods. [Color figure can be viewed in the online issue, which is available at wileyonlinelibrary.com.]

annealed freeze-dry samples prepared with/without a proper aggregation step exhibited a I_{620}/I_{570} ratio of ~ 1.07 (All curves in Fig. 5), which indicated a very similar morphology after thermal annealing.

The nonannealing fibers of P3HT prepared from polar and high boiling solvent are very fine and disorder. Upon thermal treatment, local aggregation occurs between the side chains^{41,42} and creates an order structure with a small domain size. From this study, we found freeze-dry samples maintained their original aggregated states in gel form, which was a continuous structure in three-dimensions and an order structure of a large domain size.

Photoluminescence study

The photoluminescence (PL) spectra of spin-coating and freeze-dry samples were shown in Figure 7. The spin-coating sample displayed a PL emission peak at 675 nm [Fig. 7(a)], which was 37 nm lower than that of the freeze-dry sample that appeared at 712 nm [Fig. 7(b)]. This result indicated that the extent of π - π stacking between P3HT molecules in the freeze-dry samples were much stronger than that in the

spin-coating samples. Figure 7(a) showed the PL spectra of the spin-coating samples that were annealed at 150°C for different periods of time. No major change could be observed for these PL spectra even when the annealing period was prolonged to 60 min. For the samples that were prepared by the freeze-dry method, we did observe a slight bathochromic shift (~ 7 nm) due to the aggregation of P3HT after annealing for 60 min [Fig. 7(b)]. Evidently, the change in aggregation states for P3HT molecules in freeze-dry samples was larger than those prepared by spin-coating. As mentioned in the previous paragraph, P3HT molecules in spin-coating films were arranged with a disorder structure before annealing and only short-range order structure could be obtained after thermal annealing. However, P3HT molecules formed a loose but order structure in the freeze-dry films before annealing and they form compact and order structure after annealing.

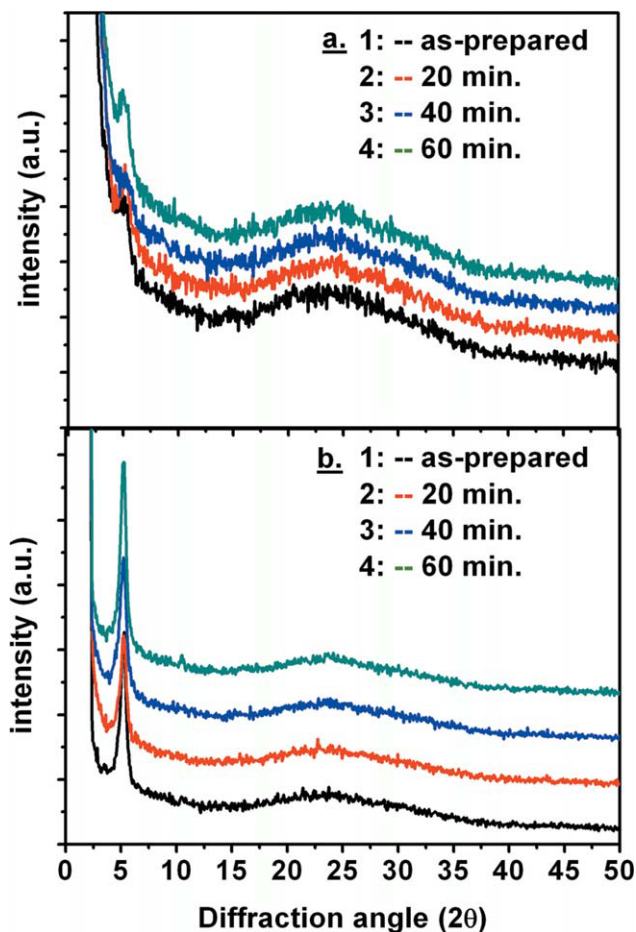


Figure 8 X-ray diffraction patterns of the nonannealed and annealed P3HT films prepared by the freeze-dry method with different lengths of aggregation time, (a) nonannealed and (b) annealed films (annealing conditions: 150°C for 30 min). [Color figure can be viewed in the online issue, which is available at wileyonlinelibrary.com.]

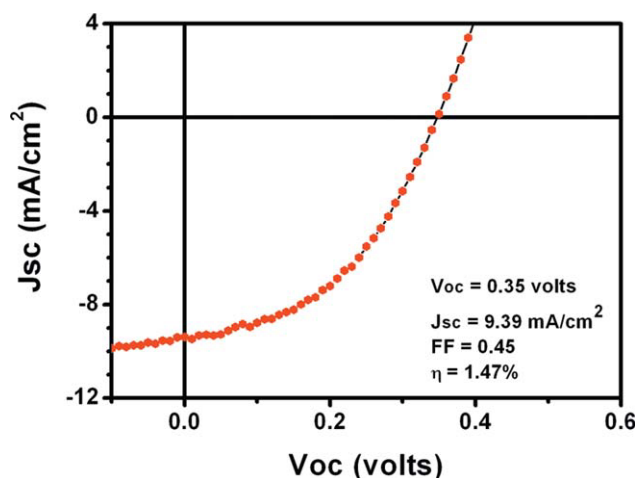


Figure 9 I–V curve and device properties of a prototype polymer solar cell prepared by freeze-dry method without optimization. Device configuration of the solar cell is ITO/PEDOT : PSS (800 Å)/P3HT : PCBM (1000 Å)/Ca(25 Å)/Al(2000 Å). [Color figure can be viewed in the online issue, which is available at wileyonlinelibrary.com.]

X-ray analysis

X-ray diffraction patterns of the freeze-dry samples and their respective annealed samples were depicted in Figure 8. As shown in Figure 8(a), the nonannealed samples displayed a gradual increase in the intensity of the peak located at $2\theta = 5.1^\circ$, which was attributed to the aggregation of alkyl side chains¹⁸ during the aggregation period. A moderate increase in the height of this peak confirmed the effect of the length of the aggregation period on the alignment of the alkyl side chains. This conclusion is further confirmed by the annealing study [Fig. 8(b)]. All freeze-dry samples exhibited a very sharp diffraction peak at $2\theta = 5.1^\circ$ upon annealing at 150°C for 30 min. These results were in consistent with the absorption and the photoluminescence studies mentioned above (Figs. 5 and 7).

All the experimental results confirmed that the organization of P3HT molecules within the dried P3HT fiber prepared by the freeze-dry method was an ordered and connected structure upon thermal annealing. The degree of order did not vary with different aggregation periods after thermal treatment. Therefore, the P3HT fibers prepared by freeze-dry process followed by thermal treatment should be with consistent properties and should be suitable for solar cell applications. The concept of creating an order and connected P3HT network followed by applying PCBM on the surface of the connected P3HT fibers for solar cells application is important because of a bicontinuous phase formation with less phase separation issue. A prototype polymer solar cell was fabricated with the film prepared by freeze-dry process as described in the experimental section.

Figure 9 showed the device performance of the solar cell with the device configuration of ITO/PEDOT : PSS (800 Å)/P3HT : PCBM (1000 Å)/Ca(25 Å)/Al(2000 Å). A power conversion efficiency of 1.47% could be achieved for the prototype solar cell without further thermal annealing. Although the open circuit voltage (V_{oc}) and the fill factor (FF) were both low, short circuit current density (J_{sc}) of the device was comparable to that reported in literature.⁴³ The pore size of the P3HT film was not optimized and the device was not thermally treated after coating of PCBM. As reported in literatures, thermal annealing will enhance device properties such as V_{oc} and J_{sc} . Therefore, V_{oc} and J_{sc} of this prototype device shall be higher after appropriate thermal annealing.

CONCLUSIONS

A porous network structure of P3HT aggregates was obtained by employing a freeze-dry process. A SEM microgram showed that the dimensions of the P3HT aggregates could be controlled by different periods of aggregation time. The absorption study indicated that the freeze-dry films exhibited higher degree of order structure between thiophene molecules than those of the spin-coating films. In addition, the absorption spectra revealed that the microstructure of P3HT aggregates obtained from a suitable aggregation process and freeze-dry treatment was very similar upon annealing at 150°C for 30 min. Photoluminescence study showed a large difference in emission peak (~ 37 nm) for the freeze-dry sample (at 712 nm) as compared with that of the spin-coating sample (at 675 nm). This result again confirmed that the extent of π - π stacking between P3HT molecules in the freeze-dry samples were much stronger than those in the spin-coating samples. X-ray analysis showed that all the annealed freeze-dry samples exhibited a very sharp diffraction peak at $2\theta = 5.1^\circ$ with high intensity, which was the characteristic peak for the side chain aggregation of P3HT molecules. All evidences verified that the freeze-dry P3HT film was an order and connected structure. For P3HT film with such consistent properties, a prototype solar cell was fabricated with a PCE of 1.47% without further optimization.

PT would like to thank Professor S.N. Lee of the department for proofreading this article.

References

1. Padinger, F.; Rittberger, R. S.; Sariciftci, N. S. *Adv Funct Mater* 2003, 13, 85.
2. Kim, J. Y.; Kim, S. H.; Lee, H. H.; Lee, K.; Ma, W.; Gong, X.; Heeger, A. J *Adv Mater* 2006, 18, 572.
3. Bao, Z.; Dodabalapur, A.; Lovinger, A. *J Appl Phys Lett* 1996, 69, 4108.

4. Erb, T.; Zhokhavets, U.; Gobsch, G.; Raleva, S.; Stuhn, B.; Schilinsky, P.; Waldauf, C.; Brabec, C. J. *Adv Funct Mater* 2005, 15, 1193.
5. Savenije, T.; Kroeze, J.; Yang, X.; Loos, J. *Adv Funct Mater* 2005, 15, 1260.
6. Salleo, A.; Chen, T. W.; Volkel, A. R.; Liu, P.; Ong, B. S.; Street, R. A. *Phys Rev B Condens Matter Mater Phys* 2004, 70, 115311.
7. Veherac, J. M.; Leblevenec, G.; Djurado, D.; Rieutord, F.; Chouiki, M.; Travers, J. P.; Pron, A. *Synth Met* 2006, 156, 815.
8. Brinkmann, M.; Rannou, P. *Adv Funct Mater* 2007, 17, 101.
9. Schilinsky, P.; Asawapirom, U.; Scherf, U.; Biele, M.; Brabec, C. *J Chem Mater* 2005, 17, 2175.
10. Kim, Y.; Cook, S.; Tuladhar, S. M.; Choulis, S. A.; Nelson, J.; Durrant, J. R.; Bradley, D. D. C.; Giles, M.; McCulloch, I.; Ha, C. S.; Ree, M. *Nat Mater* 2006, 5, 197.
11. Urien, M.; Bailly, L.; Vignau, L.; Cloutet, E.; Cuendias, A.; Wantz, G.; Cramail, H.; Hirsch, L.; Parneix, J. P. *Polym Int* 2008, 57, 64.
12. Kim, Y.; Cook, S.; Kirkpartrick, J.; Nelson, J.; Durrant, J. R.; Bradley, D. D. C.; Giles, M.; Heeney, M.; Hamilton, R.; McCulloch, I. *J Phys Chem C* 2007, 111, 8137.
13. Shaheen, S. E.; Brabec, C. J.; Sariciftci, N. S.; Padinger, F.; Fromherz, T.; Hummelen, J. C. *Appl Phys Lett* 2001, 78, 841.
14. Yang, H.; Shin, T.; Yang, L.; Cho, K.; Ryu, C. Y.; Bao, Z. *Adv Funct Mater* 2005, 15, 671.
15. Lee, J. K.; Ma, W. L.; Brabec, C. J.; Yuen, J.; Moon, J. S.; Kim, J. Y.; Lee, K.; Bazan, G.; Heeger, A. J. *J Am Chem Soc* 2008, 130, 3619.
16. Li, G.; Shrotriya, V.; Huang, J.; Yao, Y.; Moriarty, T.; Emery, K.; Yang, Y. *Nat Mater* 2005, 4, 864.
17. Kim, D. H.; Park, Y. D.; Jang, Y.; Kim, S.; Cho, K. *Macromol Rapid Commun* 2005, 26, 834.
18. Yang, C. Y.; Heeger, A. J. *Synth Met* 1996, 83, 85.
19. Groves, C.; Reid, O. G.; Ginger, D. S. *Acc Chem Res* 2010, 43, 612.
20. Ruseckas, A.; Shaw, P.; Samuel, I. D. W. *Dalton Trans* 2009, 45, 10040.
21. Nieuwendaal, R. C.; Snyder, C. R.; Kline, R. J.; Lin, E. K.; VandarHart, D. L.; DeLongchamp, D. M. *Chem Mater* 2010, 22, 2930.
22. Berson, S.; Bettignies, R. D.; Bailly, S.; Guillerez, S. *Adv Funct Mater* 2007, 17, 1377.
23. Prosa, T. J.; Winokur, M. J.; Moulton, J.; Smith, P.; Heeger, A. J. *Macromolecules* 1992, 25, 4364.
24. Zhao, Y.; Xie, Z.; Qu, Y.; Geng, Y.; Wang, L. *Appl Phys Lett* 2007, 90, 043504.
25. Miller, S.; Fanchini, G.; Lin, Y. Y.; Li, C.; Chen, C. W.; Su, W. F.; Chowalla, M. *J Mater Chem* 2008, 18, 306.
26. Zhang, C.; Tong, S. W.; Jiang, C.; Kang, E. T.; Chan, D. S. H.; Zhu, C. *Appl Phys Lett* 2008, 93, 043307.
27. Reyes, M.; Kim, K.; Carroll, D. L. *Appl Phys Lett* 2005, 87, 083506.
28. Sun, S. S.; Sariciftci, N. S. *Organic Photovoltaics: Mechanism, Materials, and Devices*; Taylor & Francis: London, 2005.
29. Brabec, C. J.; Dyakonov, V.; Parisi, J.; Sariciftci, N. S. *Organic Photovoltaics: Concepts and Realization*; Springer-Verlag: Heidelberg, 2003.
30. Huang, Y. C.; Chuang, S. Y.; Wu, M. C.; Chen, H. L.; Chen, C. W.; Su, W. F. *J Appl Phys* 2009, 106, 034506.
31. Chiu, M. Y.; Jen, U. S.; Su, C. H.; Liang, K. S.; Wei, K. H. *Adv Mater* 2008, 20, 2573.
32. Verilhac, J.; Leblevenec, G.; Djurado, D.; Rieutord, F.; Chouiki, M.; Travers, J.; Pron, A. *Synth Met* 2006, 156, 815.
33. Loewe, R. S.; Ewbank, P. C.; Liu, J.; Zhai, L.; McCullough, R. D. *Macromolecules* 2001, 34, 4324.
34. Chen, T. A.; Rieke, R. D. *J Am Chem Soc* 1992, 114, 10087.
35. Hoppe, H.; Niggemann, M.; Winder, C.; Kraut, J.; Hiesgen, R.; Hinsch, A.; Meissner, D.; Sariciftci, N. S. *Adv Funct Mater* 2004, 14, 1005.
36. Huang, W. Y.; Huang, P. T.; Han, Y. K.; Lee, C. C.; Hsieh, T. L.; Chang, M. Y. *Macromolecules* 2008, 41, 7485.
37. Yamamoto, T.; Komarudin, D.; Arai, M.; Lee, B. L.; Suganuma, H.; Asakawa, N.; Inoue, Y.; Kubota, K.; Sasaki, S.; Fukuda, T.; Matsuda, H. *J Am Chem Soc* 1998, 120, 2047.
38. Yue, S.; Berry, G. C.; McCullough, R. D. *Macromolecules* 1996, 29, 933.
39. Shibaev, P. V.; Schaumburg, K.; Bjornholm, T.; Norgaard, K. *Synth Met* 1998, 97, 97.
40. Spano, F. C. *Acc Chem Res* 2010, 43, 429.
41. Joshi, S.; Grigorian, S.; Pietsch, U. *Phys Stat Sol* 2008, 205, 488.
42. Ma, W.; Yang, C.; Gong, X.; Lee, K.; Heeger, A. J. *Adv Funct Mater* 2005, 15, 1617.
43. Chang, M. Y.; Chen, Y. F.; Tsai, Y. S.; Chi, K. M. *J Electrochem Soc* 2009, 156, B234.